

MICROMECHANICS MEASUREMENTS APPLIED TO INTEGRATED CIRCUIT MICROELECTRONICS

DAVID R. CLARKE
Materials Department, College of Engineering
University of California, Santa Barbara, CA 91360-5050

ABSTRACT

As in other engineered structures, fracture occasionally occurs in integrated microelectronic circuits. Fracture can take a number of forms including voiding of metallic interconnect lines, decohesion of interfaces, and stress-induced microcracking of thin films. The characteristic feature that distinguishes such fracture phenomena from similar behaviors in other engineered structures is the length scales involved, typically micron and sub-micron. This length scale necessitates new techniques for measuring mechanical and fracture properties. In this work, we describe non-contact optical techniques for probing strains and a microscopic "decohesion" test for measuring interface fracture resistance in integrated circuits.

KEYWORDS

Interconnect strains, piezospectroscopy, thin film decohesion.

INTRODUCTION

One of the key features of high-performance, integrated microelectronics is the widespread use of multi-levels of metallization and dielectrics for high-density signal and power distribution. Integrity of the interfaces between the various levels of metallization and dielectric is an essential pre-requisite since interface failure directly impacts both the manufacturing yield and the long-term reliability of the device. It is thus of major importance affecting, in one way or another, the entire semiconductor industry.

Interface failure can take a number of different forms but usually involves the decohesion of the interface over some area and the local separation of the materials on either side of the interface. In practice, decohesion commonly occurs as a result of either poor adhesion between materials, often caused by improper processing, or by the build-up of stresses within the thin-film structure. The latter can occur, for instance, as a consequence of differences in thermal expansion during processing and subsequent thermal cycling during device operation. Stresses can also accumulate as a result of electromigration driven diffusion. As new device structures are being devised for ever higher performance, feature sizes become smaller with consequentially higher stresses and higher current densities. As a result the driving forces for interface failure are also steadily increasing. In this work, we review on-going experiments designed to measure, non-destructively, local stresses associated with interconnects as well as measurements of interface decohesion using a thin-film technique utilizing the same microfabrication technology used to make integrated circuits.

PIEZOSPECTROSCOPIC MEASUREMENT OF LOCAL STRAINS

It has become routine to measure strains in thin-films by X-ray diffraction. However, in most integrated circuits, the features are not continuous films but rather narrow lines and pads. Furthermore, they are usually constrained by overlayers and different levels of metallization and dielectrics. For these reasons it is necessary to be able to probe the strains in, and around, features and simultaneously also image them. Optical microscope based techniques provide such "real space" capabilities, especially those utilizing the piezospectroscopic properties of materials. (Piezospectroscopy is the shift in spectra produced by strain.) Two characteristic spectroscopies have been used, Raman spectroscopy (DeWolf et al., 1992; Ma et al., 1995a) and fluorescence spectroscopy (Ma and Clarke, 1993; Wen, Ma and Clarke, 1995). The former spectroscopy is suited to measurements in silicon whereas the latter is suited to high-precision measurements in dielectrics, in particular to sapphire. In both cases, a laser beam is focused down to a diffraction-limited probe in an optical microscope and positioned onto features in the image of interest. The laser is used to excite a Raman spectrum or a fluorescence spectrum from the region probed. This is shown schematically in fig.1 for probing the strains around a passivated interconnect on a silicon substrate.

Although in many instances it is the strains in the substrate and the dielectrics that are of principal concern, there are a number of contemporary questions regarding the strains in various metallizations, for instance the strains in interconnects produced by thermal expansion mismatch after fabrication and the strains produced by electromigration. Although the spectra from typical metallizations are very weak or nonexistent, the strains in the metal features can nevertheless be obtained from the constraint strains induced in the adjoining substrate or the surrounding dielectric. The strains in the metallization must then be deduced from detailed comparisons between finite element computations of the fringing strain field and the spectroscopic measurements (Ma et al., 1995a; He et al., 1996). Whilst this has proven possible, the weakness of the method lies in the fact that the fringing fields vary rapidly with distances of the order of the optical probe size and hence detailed deconvolutions are essential. This is shown by the example in fig. 2 which compares the measured Raman shifts across a 3 μm wide aluminum line with those calculated for an elastic-perfectly plastic material (solid line) and after convolution with the actual probe size. Although the fit between the data and calculations is quite close, equally good fits are obtained if the hydrostatic stress is scaled by $\pm 15\%$ from the experimentally determined value of 210 MPa (Ma et al., 1995a).

To overcome these limitations, it is necessary to probe *through* the substrate and measure the strains induced directly under metallizations since these strains vary slowly with position. This cannot be done in the configuration shown in fig.1 because both the metal and the silicon substrate are opaque at frequencies in the visible. To circumvent these restrictions, we have fabricated circuit elements on c-axis oriented sapphire substrates which have a thin-film sensor fabricated on their top surface. This is shown schematically in fig. 3. The sensor part is an epitaxially grown thin-film of Cr-doped sapphire (ruby) that fluoresces when excited with a probing laser. Because the ruby film can be grown to a controlled thickness, typically 20-50 nm, it only senses strains within this distance of the top surface of the substrate. As a result it is sensitive to strains at the interface with features deposited on top of the substrate.

The piezospectroscopic shift, $\Delta\nu$, of the ruby R-line fluorescence lines is related to the stress in the probed region of a c-axis oriented sapphire single crystal by

$$\Delta\nu = \Pi_a(\sigma_{11} + \sigma_{22}) + \Pi_c\sigma_{33}$$

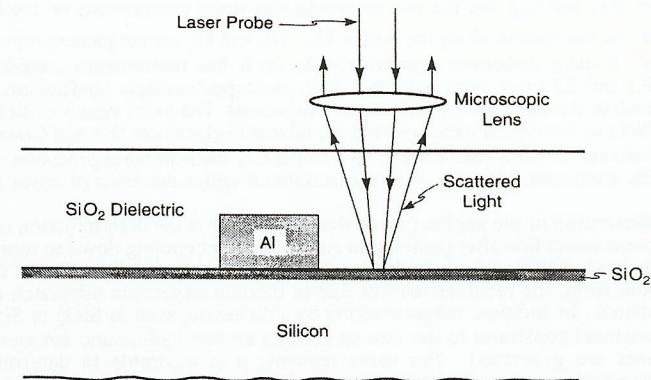


Fig.1. Optical arrangement for probing the local strains around interconnect features on a Si substrate. (Cross-section.) The optics are part of a standard optical microscope but with an attached spectrometer for analyzing the excited Raman signal used for piezospectroscopic measurements.

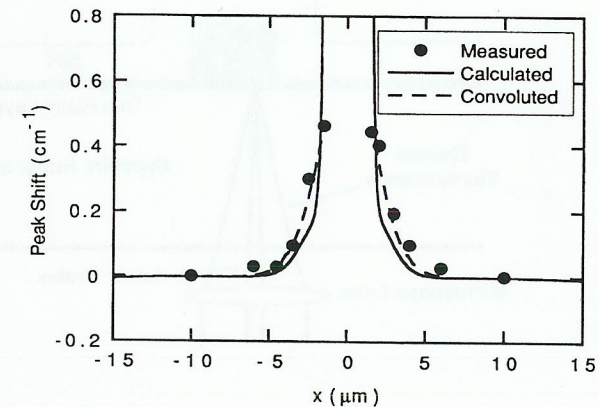


Fig. 2. Comparison between the measured and calculated Raman shift across a passivated 3 micron wide aluminum interconnect line on silicon. The calculated piezospectroscopic frequency shift distribution is further convoluted with the laser beam intensity function for the final comparison.

where σ_{11} and σ_{22} are the two perpendicular stress components on the basal plane and σ_{33} is the stress component along the c -axis. Π_a , Π_b and Π_c are the piezospectroscopic coefficients for the a , b and c directions respectively. As the R-line fluorescence consists of two distinct lines, the R1 and R2 lines, each with their own piezospectroscopic coefficients it is possible to solve for each of the three orthogonal stress components. The exact values of all the piezospectroscopic coefficients have been measured and are tabulated elsewhere (He and Clarke, 1995). The values are between 2 and 3 $\text{cm}^{-1} \text{GPa}^{-1}$, so a frequency measurement precision of 0.05 cm^{-1} , which is readily attainable, provides stress measurements with a precision of about 20 MPa.

An illustration of the application of the ruby sensor is the determination of the residual stress in an interconnect line after passivation and subsequent cooling down to room temperature. As the yield stress of fine-scale metal features is known to be generally different from the same metal in its bulk form, the residual stresses due to thermal expansion mismatch cannot be confidently calculated. In addition, the passivation by a dielectric, such as SiO_2 or Si_3N_4 , provides a three-dimensional constraint to the line on cooling so that hydrostatic stresses as well as deviatoric stresses are generated. For these reasons, it is desirable to determine the strains in an interconnect, compare them with computations and hence establish the appropriate constitutive behavior for the metal for subsequent analyses.

Figure 3 is an example of the fluorescence frequency shifts measured across a fully passivated aluminum line and the corresponding stresses calculated from the shifts. The aluminum line, 2.3 micron wide and 2 micron high, was produced by a standard lithography and evaporation procedure. It was then heated to 350°C for the deposition of 2 microns of SiO_2 passivation and

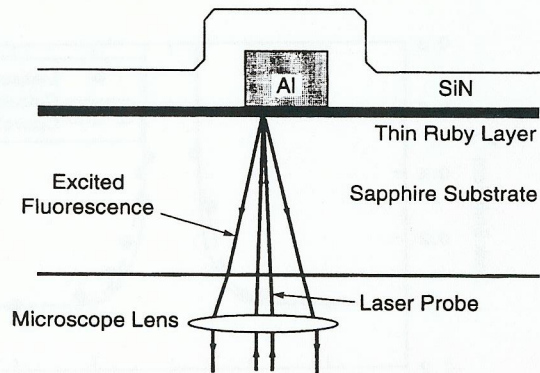


Fig. 3. Optical arrangement for probing the strains induced in a thin (~50nm) ruby sensor by an interconnect structure deposited on the ruby sensor. The strain is measured by the piezospectroscopic shift of the Cr^{3+} fluorescence from the ruby. The arrangement enables the strain field directly under a feature to be probed as well as the fringing field at the edges.

finally annealed for 3 hours at the same temperature to develop a "bamboo" grain structure. Although a detailed comparison with finite element computations is necessary to determine the stress field within the interconnect from these shifts the continuity of stress perpendicular to the interconnect/substrate interface requires that σ_{zz} has a value of 400 MPa, the value given by the intercept at $x=0$ in the figure. Stresses this high indicate a significant level of hydrostatic stress. A full analysis is in preparation.

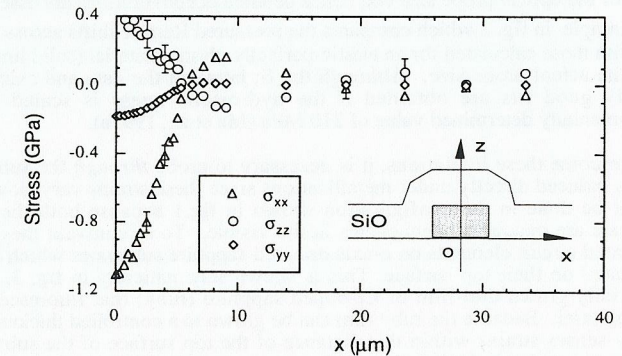
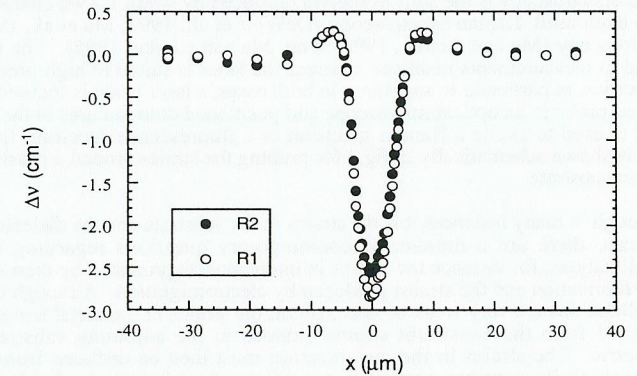


Fig. 4. Top. Cr^{3+} fluorescence frequency shift of the R1 and R2 lines as a function of distance across a fully passivated 2.3 micron wide and 2 micron thick aluminum interconnect line. The SiO_2 passivation was deposited at 350°C and annealed for 3 hours prior to cooling to facilitate grain growth. Bottom. The corresponding thermal expansion induced stress components in the sapphire substrate within 50 nm of the surface.

INTERFACE DECOHESION

The basic phenomena underlying interface decohesion have been identified during the course of the last two or three decades. Amongst the most important are the stress in the film, σ_f , the role of the interface decohesion energy, Γ_i , and its dependence on the loading mixity, Ψ . In contrast to the evolving understanding of interface decohesion, techniques for the measurement of decohesion have not advanced significantly. Most tests are, in reality, comparison tests, such as the "peel" and "scratch" tests. Although simple to apply, useful for comparative purposes, and capable of identifying instances of particularly poor adhesion, they are neither quantitative nor can the important fracture mechanics parameters mentioned above be controlled. As a result there is an industry-wide need to quantitatively measure the decohesion energy of interfaces created in device fabrication rather than model systems. Furthermore, such a quantitative test is an essential step towards the design of "back-end-of-the-line" processes that also optimize the strength of interfaces. A recently developed technique, utilizing microfabrication-based thin-film technology, provides one approach to direct measurement of interface decohesion. In its original implementation (Bagchi et al., 1994) it was applied to interfaces in simple model systems consisting of a thin film evaporated onto a glass or polymer substrate. In this work, the technique is extended to device interfaces in multilayer structures produced by standard semiconductor processing.

The Physical Basis of the Decohesion Test:

Decohesion of an interface commonly occurs as a result of the build-up of residual stresses in the thin films forming the interface. Spontaneous decohesion occurs when the strain energy release rate, G , accompanying the advance of the delaminated region (the interfacial crack in fig.5) exceeds the interfacial energy, Γ_i , namely when $G > \Gamma_i$. For the simplest case of a thin film strip subject to a residual tension, σ_f , on a thick substrate, fracture mechanics analysis shows that decohesion will be energetically favored when:

$$G = \frac{\sigma_f^2 h_f}{E_f} \geq \Gamma_i$$

where E_f is the Young's modulus of the film and h_f is the film thickness. This equation indicates that decohesion will take place when the thickness of a stressed film exceeds a critical value.

The basis of the thin-film decohesion test is to mimic these conditions by increasing the residual stress and the film thickness by depositing onto the thin-film structure of interest a superlayer -- a "stressor" -- of a material having a large intrinsic stress, such as Cr. (Fig 5). By systematically varying the thickness of the superlayer, the driving force for decohesion is increased until a critical thickness of the superlayer is attained at which spontaneous decohesion occurs. Because of the imbalance of the residual stresses in the film and "stressor", a bending moment exists and so once the critical thickness is exceeded the film "curls up" away from the substrate. By using elasticity solutions for residually stressed films the interfacial fracture resistance may be obtained from the decohesion condition:

$$G = \frac{\sigma_f^2 h_f}{E_f} + \left(\frac{\sigma^2 h}{E} \right)_{Cr} \geq \Gamma_i$$

In performing the test a blanket "stressor" film is first deposited on the features of interest and then long strips of the film are created lithographically and removing, by reactive ion etching or sputtering, the adjacent regions. If the decohesion condition above is exceeded, the interface will decohere and the strip will then curl up. If the condition is not satisfied, then the strip will not curl up. So, by systematically repeating the test with different thicknesses of the "stressor" the decohesion energy may be identified from the minimum thickness that just causes decohesion.

The other parameter, the film stress, σ_f , required to obtain quantitative values can be determined independently by wafer curvature measurements, X-ray diffraction measurements of the lattice parameter or, as described above, piezospectroscopically.

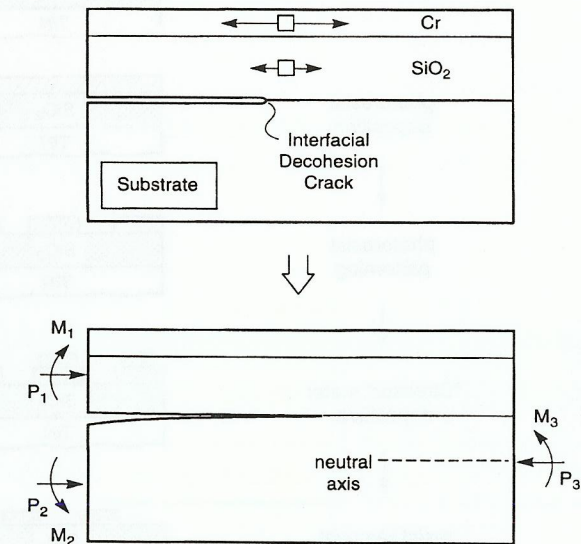


Fig. 5. Schematic diagram of the stresses driving an interfacial decohesion crack and the corresponding forces and moments acting on the film. The overlayer of Cr increases the elastic strain energy in the film and provides an additional driving force for decohesion of the strip at the interface shown. Once decohesion is initiated the net bending moment causes the film to curl up as shown later in fig. 7.

Process Implementation

One of the commonest interfaces in present microprocessors is that between SiO_2 and TiN. Since this interface generally is formed as part of a multilayer stack a lithographic process is required to not only create the "stressor" strips but also to etch down in a multilayer stack so as to subsequently cause decohesion to occur along the desired SiO_2/TiN interface. The processing scheme adopted is shown schematically in fig. 6. The result is a series of parallel strips of chromium coated SiO_2 which, because of the stored elastic strain energy, stresses the SiO_2/TiN interface.

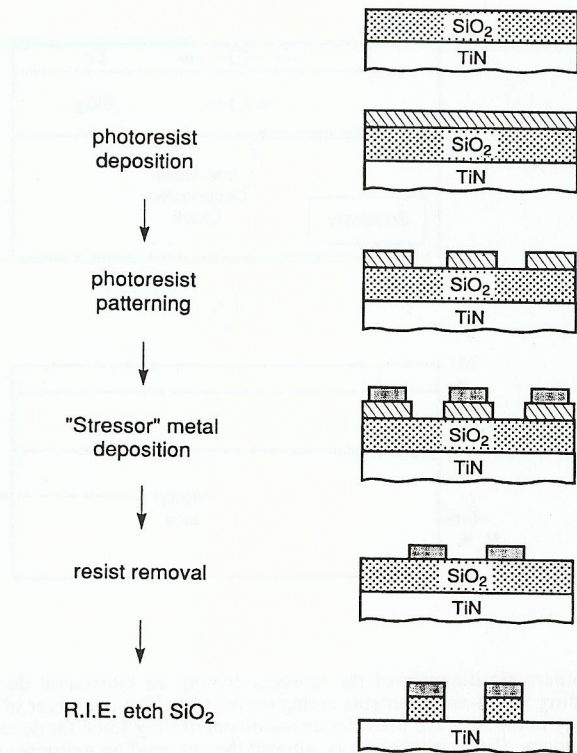


Fig. 6. Processing scheme for producing narrow strips of Cr on a SiO_2 dielectric having an interface with an underlying TiN film. The TiN film is on top of a Al metal layer in a multilayer stack (details not shown).

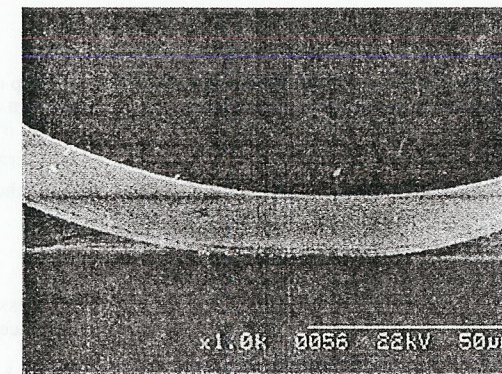
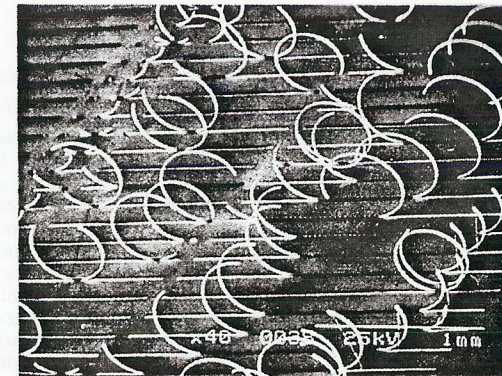


Figure 7. (Top). General view of a series of decohering 20 micron wide Cr/ SiO_2 strips. The strips typically decohere from each end and "unzip" as a function of time until the tips of the decohered regions reach an equilibrium spacing as shown in the bottom scanning electron micrograph.

As an example of the viability of the decohesion test, two different interfaces, previously fabricated at Intel Corp. were compared. Both were multilayer stacks on silicon with a series of $\text{SiO}_2/\text{TiN}/\text{Ti}/\text{Al}/\text{SiO}_2$ layers but had been deposited under different conditions. One set of conditions led to a "good" interface and the other led to a "poor" interface. To test these interfaces, a series of chromium depositions were carried out on each sample until the critical thickness for spontaneous decohesion was identified. Once the critical thickness was exceeded, the chromium strips decohered as could be seen under the optical microscope and subsequently by scanning electron microscopy. An example is shown in fig. 7. From the observed critical thickness and the measured residual stress in the chromium strips, the decohesion energies were calculated using the mechanics outlined above and listed in Table I. For comparison, the interfacial fracture energies obtained at Intel using a bulk four-point flexure test in which a crack is propagated along one of the $\text{SiO}_2/\text{TiN}/\text{Al}$ interfaces formed when two silicon substrates are diffusion-bonded together at the interfaces are also shown (Ma et al., 1995b).

Table I. Comparison of Interfacial Decoherence Energies

Sample	Interfacial Decoherence Energy (Jm^{-2})	
	Thin Film Test Critical Thickness Criterion	Bulk Test Four Point Bending (Ma et al., 1995b)
A ("Good")	14.5 ± 1.0	13.0
B ("Poor")	8.5 ± 1.0	8.1

Interface Fracture Energy From The Equilibrium Attached Length

The utilization of the thin-film decohesion test as described has a serious, practical limitation. It is that a series of tests, each with a different thickness of the "stressor" film is required to bound the interface fracture resistance. Since each test involves a series of lithographic, deposition and etching steps, the determination of the fracture resistance can be an involved and time-consuming operation. An alternative approach stems from the observation that once the critical thickness was exceeded, the strips generally decohered from both ends and the two decohesion cracks propagated towards one another until they stopped at a constant separation. This separation distance provides an alternative measurement of the decohesion energy. Finite element calculations (He, unpublished) indicate that as two decohesion cracks approach one another they stop at a finite distance that is dependent on the film thickness, the film stress, the strain energy release rate and the constitutive elastic and plastic properties of the materials. Under equilibrium conditions, the two decohesion cracks stop when the strain energy release rate is equal to the interface decohesion energy. The finite element computations for the particular case of a 1 micron thick chromium "stressor" layer decohering a $1 \mu\text{m}$ SiO_2 layer from a TiN layer is shown in the graph of fig. 8 for a fully elastic solution. Similar curves have been calculated for the case in which the metal layer underlying the TiN is a work-hardening material rather than being elastic.

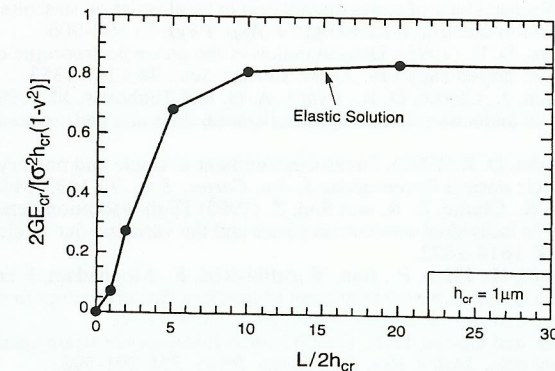
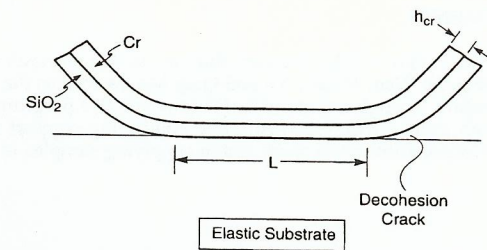


Figure 8. As two decohering ends of a residually stressed strip approach one another the driving force decreases until they stop at an equilibrium distance, L . (Top figure. Not to scale). The distance is dependent on the film stress, σ_f , the crack driving force, G , and the elastic modulus, E , as indicated by the results of the finite element computations in the lower figure.

Evidence For Environmental Assisted Interface Decohesion

During the course of experiments on the SiO_2/TiN interface, one of the unexpected observations made in the initial tests was that once the strips exceeded the critical thickness, they continued to decohere slowly rather than "unzip" spontaneously. Indeed, in some instances they continued for hours and days after lift-off had been completed. This behavior suggests that the SiO_2/TiN interface decohesion is a time-dependent phenomenon and such a phenomenon, although well-known in the ceramics literature, had not previously been reported for actual interfaces commonly produced in the microelectronics industry. In very dry atmospheres, no time-dependent decohesion is observed whereas in high humidity atmospheres continued decohesion occurs. For this reason, detailed, time-dependent measurements of the intact length as a function of partial pressure of water vapor are presently underway.

ACKNOWLEDGMENTS

It is a pleasure acknowledge the contributions to this research area from Stefanie Chiras, Deirdre Ragan, Qingzhe Wen, Jessica Xu and Qing Ma, as well as the financial support for them from Intel Corporation through a State of California MICRO program and the National Science Foundation through grant CMS-9625796. The continuing support from Harry Fujimoto and Qing Ma of Intel Corporation in this work and in supplying samples is also appreciated.

REFERENCES

- Bagchi, A., Lucas, G.E., Suo, Z. and Evans, A.G. (1994). A new procedure for measuring the decohesion energy for thin ductile films on substrates. *J. Mater. Res.* **9** 1734-1741.
- DeWolf, I., Vanhellemont, J., Romano-Rodriguez, A., Norstrom, H. and Maes, H. E. (1992) Micro-Raman study of stress distribution in local isolation structures and correlation with transmission electron microscopy. *J. App. Phys.* **71** 898-906.
- He, J. and Clarke, D. R. (1995). Determination of the piezospectroscopic coefficients of chromium doped sapphire. *J. Am. Ceram. Soc.*, **78** 1347-1353.
- He, M.Y., Lipkin, J., Clarke, D. R., Evans, A. G. and Tenhover, M. (1996) Residual stresses in dielectrics caused by metallization lines and pads. *Acta Mater.* **44** 2353-2359.
- Ma, Q. and Clarke, D. R. (1993). Stress measurement in single and polycrystalline ceramics using their optical fluorescence. *J. Am. Ceram. Soc.*, **76** 1433-1440.
- Ma, Q., Chiras, S., Clarke, D. R. and Suo, Z. (1995) High resolution determination of the stresses in individual interconnect lines and the variation due to electromigration. *J. App. Phys.* **78** 1614-1622.
- Ma, Q., Fujimoto, H., Flinn, P., Jain, V., Adibi-Rizi, F., Moghadam, F and Dauskardt, R. H. (1995) Quantitative measurement of interface fracture energy in multilayer thin-film structures. *Mater. Res. Soc. Symp. Proc.*, **391** 91-96.
- Wen, Q., Ma, Q. and Clarke, D. R. (1995) In-situ fluorescence strain sensing of the stress in interconnects, *Mater. Res. Soc. Symp. Proc.*, **356** 591-596.